

---

---

**Universiteit Utrecht**



*Mathematics  
Institute*

**The Cauchy-Riemann equations: discretization  
by finite elements, fast solution, and a posteriori  
error estimation**

by

**Jan Brandts**

---

---

Preprint

No. 1179

January, 2001

Also available at URL <http://www.math.uu.nl/people/brandts>

---

---

# The Cauchy-Riemann equations: discretization by finite elements, fast solution, and a posteriori error estimation

Jan Brandts\*

January, 2001

## Abstract

In this paper we will concentrate on the numerical solution of the Cauchy-Riemann equations. First we show that these equations bring together the finite element discretizations for the Laplace equation by standard finite elements on the one hand, and by mixed finite element methods on the other. As a consequence, methods for a posteriori error estimation for both finite element methods can derive their validity from each other. Moreover, we show that given a finite element approximation of one of the vectorfields, the missing can be accurately computed in optimal complexity.

**Keywords:** Cauchy-Riemann equations, Laplace problem, superconvergence, post-processing, error estimation, marching process, optimal complexity.

**AMS subject classification:** 65N30.

## 1 Introduction

The ordered pair  $(u, v)$  of functions defined on some domain  $\Omega \subset \mathbb{R}^2$  is said to satisfy the *Cauchy-Riemann equations* in  $\Omega$  if  $\nabla u = \mathbf{curl} v$  in  $\Omega$ , which, written out in partial derivatives, reads as

$$\frac{\partial}{\partial x}u = \frac{\partial}{\partial y}v \quad \text{and} \quad \frac{\partial}{\partial y}u = \Leftrightarrow \frac{\partial}{\partial x}v \quad \text{in } \Omega. \quad (1)$$

For ease of explanation, we will also say that  $(v, u)$  satisfies the Cauchy-Riemann equations, even though the pair  $(\Leftrightarrow v, u)$ , rather than  $(v, u)$ , satisfies (1).

The Cauchy-Riemann equations have not been the study of numerical approximation extensively. Nonetheless, already in 1979, Ghil et al. [9] developed a finite difference scheme on rectangular domains that is as efficient as a fast Poisson solver, whereas in the context of elliptic systems, the Cauchy-Riemann equations were taken as a first model problem by Brandt et al. in [3]. A fairly recent paper by Borzi et al. [1] considers a multilevel approach with cell-vertex finite volumes on a square domain. The papers just mentioned treat the general inhomogeneous equations.

---

\*Mathematical Institute, Utrecht University, Budapestlaan 6, 3584 CD, Utrecht, The Netherlands. E-mail: brandts@math.uu.nl

## 1.1 Motivation

The importance of the Cauchy-Riemann equations lies in several fields, both of theoretical and practical nature. Firstly, it is well-known that a function is complex analytic if and only if its real and complex part, seen as functions from  $\mathbb{R}^2$  to  $\mathbb{R}$ , satisfy (1). This means that if either the real or the complex part of such a function is known, a general form for the remaining part can be found by solving it from the Cauchy-Riemann equations. Secondly, an elementary practical application is that the level curves of  $u, v : \mathbb{R}^2 \rightarrow \mathbb{R}$  are mutually orthogonal if the pair  $(u, v)$  satisfy the Cauchy-Riemann equations. An example is given in Figure 1 below.

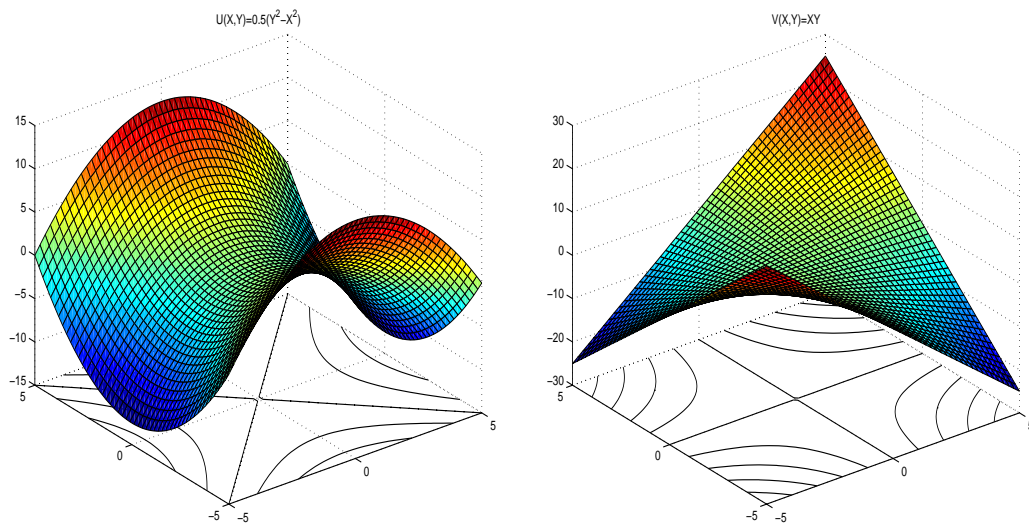


**Figure 1.** Example of a Cauchy-Riemann pair  $(u, v)$  with  $u(x, y) = \frac{1}{2}(x^2 + y^2)$  and  $v(x, y) = xy$ . Note that actually  $v$  is the function  $u$  rotated over  $\pi/4$ , i.e.,  $u(x, y) = (y \leftrightarrow x)(y + x)$ .

So, the Cauchy-Riemann equations describe the relation between isotherms and heatflow, between equipotential lines and the direction of electric force, and also between equipotential lines and the streamlines of a fluid flow. As a final motivation for the study of Cauchy-Riemann equations we recall that they are in fact the simplest example of an elliptic system and can therefore be taken as a model problem for more complicated systems. As shown in [15], they form the elliptic part of the inviscid incompressible Euler problem in two space dimensions. These applications explain our interest in fast and accurate numerical tools for their approximation.

## 1.2 Formulation of the problem and outline of the approach

Depending on the context, there are several feasible formulations of the Cauchy-Riemann problem. An example is that  $v$  is given, and that  $u$  such that  $\nabla u = \mathbf{curl} v$  is desired. In that case,  $u$  is uniquely determined up to a constant value. Another example is that both  $u$  and  $v$  are unknown, but that they satisfy (1). In that case, compatible boundary conditions for both  $u$  and  $v$  should be given, or boundary conditions sufficient to determine one of the two. In this paper, we will concentrate on both formulations, the first being a sub-problem of the second. As a model

problem, we will look for a pair of functions  $(u, v)$  with mean values zero such that

$$\nabla u = \mathbf{curl} v \text{ in } \Omega, \quad \nabla u^T \nu = j \text{ on } \partial\Omega, \quad \text{and} \quad \langle j, 1 \rangle = 0, \quad (2)$$

where  $\nu$  is the unit outer normal to  $\partial\Omega$ , and formulate this as an independent potential problem for  $u$ . It will become clear further on that also Dirichlet boundary conditions could have been posed.

Approximations  $v_h$  for  $v$  will be constructed from standard [5] finite element approximations  $u_h$  of  $u$  in (2). In case  $u$  is already known *a priori*, the same ideas can still be applied in a slightly modified form. In Section 2 it will be shown that, rather surprisingly, mixed finite element approximations  $v_h$  of  $v$  can be directly and cheaply obtained as a by-product of the computation of  $u_h$ . Finally, we concentrate on superconvergence properties of some of the discrete functions of interest. The possibilities of a *posteriori* error estimation and adaptivity turn the procedure into a complete and attractive package.

### 1.3 Notations and preliminaries

In this paper,  $\Omega$  is a convex polygonal domain such that the boundary  $\partial\Omega$  is Lipschitz-continuous. By  $H^k(\Omega)$  we denote the Sobolev space of functions with weak partial derivatives of order  $k$  in  $H^0(\Omega) := L^2(\Omega)$ , normed with  $\|\cdot\|_k$ , semi-normed with  $|\cdot|_k$ . The subspaces  $\tilde{H}^k(\Omega) \subset H^k(\Omega)$  are formed by the functions with mean value zero. The space  $\mathbf{H}(\text{div}; \Omega)$  consists of functions with weak divergence in  $L^2(\Omega)$ , and we supply it with the usual norm  $\|\cdot\|_{\text{div}}$ . The subspace  $\tilde{\mathbf{H}}(\text{div}; \Omega) \subset \mathbf{H}(\text{div}; \Omega)$  contains the vectorfields with normal traces that have zero average on  $\partial\Omega$ . By the Gauss Divergence Theorem, this means that  $\text{div } \mathbf{q} \in \tilde{L}^2(\Omega)$  for  $\mathbf{q} \in \tilde{\mathbf{H}}(\text{div}; \Omega)$ . We denote unit outer normal vectors by  $\nu$  and counterclockwise tangent vectors by  $\tau$ . To what exactly they are normal and tangent will become clear from the context. The  $L^2$  inner products on  $\Omega$  and  $\partial\Omega$  will be denoted by  $(\cdot, \cdot)$  and  $\langle \cdot, \cdot \rangle$  respectively. For volumes of edges and triangles we use the notation  $|\cdot|$ .

### 1.4 Two problems involving potentials

Problem (2) can be cast in the form of two weakly formulated potential problems. We refer to Girault and Raviart [8], Ch.1 for details on the statements concerning regularity, and start with assuming that  $u, v \in \tilde{H}^2(\Omega)$ . Then, taking the divergence of the identity  $\nabla u = \mathbf{curl} v$  results in a Laplace equation for  $u$  with Neumann boundary conditions for which it follows that  $\nabla u^T \nu = j \in H^{\frac{1}{2}}(\partial\Omega)$ ,

$$\Leftrightarrow \Delta u = 0 \text{ in } \Omega, \quad \nabla u^T \nu = j \text{ on } \partial\Omega, \quad \text{and} \quad \langle j, 1 \rangle = 0. \quad (3)$$

Similarly, taking the rotation of  $\nabla u = \mathbf{curl} v$  shows that  $\Delta v = \Leftrightarrow \text{rot } \mathbf{curl} v = \Leftrightarrow \text{rot } \nabla u = 0$ . Next, a boundary condition for  $v$  can be found by using the identities

$$\mathbf{curl} = \begin{pmatrix} 0 & 1 \\ \Leftrightarrow 1 & 0 \end{pmatrix} \nabla \quad \text{and} \quad \nu = \begin{pmatrix} 0 & 1 \\ \Leftrightarrow 1 & 0 \end{pmatrix} \tau, \quad (4)$$

which leads to

$$\frac{\partial}{\partial \tau} v = \nabla v^T \tau = \mathbf{curl} v^T \nu = \nabla u^T \nu = j. \quad (5)$$

Integration of (5) along  $\partial\Omega$  results in a Laplace equation for  $v$  with Dirichlet boundary conditions,

$$\Leftrightarrow \Delta v = 0 \text{ in } \Omega, \text{ and } v = g \text{ on } \partial\Omega, \text{ where } \frac{\partial}{\partial \tau} g = j \text{ on } \partial\Omega, \quad (6)$$

and it follows that  $g \in H^{\frac{3}{2}}(\partial\Omega)$ . Now, by the theory of elliptic regularity for the Poisson problem on convex polygonal domains, the assumed regularity  $u, v \in \tilde{H}^2(\Omega)$  can, conversely, be concluded from the assumption  $j \in H^{\frac{1}{2}}(\partial\Omega)$  on the given data, which is what we will from now on assume.

**Remark 1.1** Problem (2) has solutions  $u, v \in \tilde{H}^1(\Omega)$  if  $j \in H^{-\frac{1}{2}}(\partial\Omega)$ . However, with the upcoming lowest order finite element discretizations in mind, we prefer to have  $u, v \in \tilde{H}^2(\Omega)$  for optimal convergence.

We will use the standard finite element method with Lagrange finite elements for the approximation of  $u$ , which will give us a sequence of approximate solutions  $u_h \in \tilde{V}_h \subset \tilde{H}^1(\Omega)$  of (3). Simultaneously, we will construct mixed finite element approximations  $v_h \in \tilde{W}_h \subset \tilde{L}^2(\Omega)$  for the function  $v$ . This will be done in such a way, that each pair  $(u_h, v_h) \in \tilde{V}_h \times \tilde{W}_h$  satisfies the Cauchy-Riemann equations in a certain discrete sense. Indeed, neither  $u_h$  nor  $v_h$  is a harmonic function, but the weak partial derivatives of  $u_h$  can be interpreted as distributional derivatives of  $v_h$  on the finite dimensional space  $\tilde{W}_h$ . As  $u_h$  converges to  $u$  in  $\tilde{H}^1(\Omega)$ ,  $v_h$  converges to  $v$  in  $\tilde{L}^2(\Omega)$ . We will consider lowest-order elements only, although the procedure is easily extended to higher order elements.

## 2 Discretization by finite elements

In this section we will formulate the standard finite element method for Laplace equation (3), and apply the mixed finite element method to Laplace equation (6). We refer to Ciarlet [5] and Raviart and Thomas [14] for details on these methods.

### 2.1 Standard finite elements

Consider Equation (3). Its solution is the unique function  $u \in \tilde{H}^2(\Omega) \subset \tilde{H}^1(\Omega)$  such that for all  $y \in \tilde{H}^1(\Omega)$ ,

$$(\nabla u, \nabla y) = \langle j, y \rangle. \quad (7)$$

Denote the space of continuous, mean value zero, piecewise linear functions relative to some triangulation  $\mathcal{T}_h$  of the domain  $\Omega$  by  $\tilde{V}_h$ , where  $h$  is the usual mesh-parameter. Then the standard finite element approximation  $u_h \in \tilde{V}_h$  of  $u$  uniquely satisfies

$$(\nabla u_h, \nabla y_h) = \langle j, y_h \rangle, \quad (8)$$

for all  $y_h \in \tilde{V}_h$ , and the Galerkin orthogonality  $(\nabla(u \Leftrightarrow u_h), \nabla y_h) = 0$  obtained by subtracting (8) from (7) for testfunctions  $y_h \in \tilde{V}_h$ , expresses that  $u_h$  is the elliptic projection of  $u$  on  $\tilde{V}_h$ . The following *a priori* bound

$$\|u \Leftrightarrow u_h\|_0 + h\|u \Leftrightarrow u_h\|_1 \leq Ch^2|u|_2, \quad (9)$$

holds under the mild additional assumption that the family  $(\mathcal{T}_h)_h$  of triangulations employed, is regular, which means that there does not exist a sequence  $(T_h)_h$  with  $T_h \in \mathcal{T}_h$  such that  $\liminf_{h \rightarrow 0} \text{Vol}(T_h)h^{-2} = 0$ .

## 2.2 Mixed finite elements

The mixed weak formulation of (6) introduces a second variable  $\mathbf{p} = \Leftrightarrow \nabla v \in \tilde{\mathbf{H}}(\text{div}; \Omega)$  and treats it as an independent variable. Concretely, it seeks a pair  $(v, \mathbf{p}) \in \tilde{L}^2(\Omega) \times \tilde{\mathbf{H}}(\text{div}; \Omega)$  such that for all  $(w, \mathbf{q}) \in \tilde{L}^2(\Omega) \times \tilde{\mathbf{H}}(\text{div}; \Omega)$ ,

$$(\mathbf{p}, \mathbf{q}) \Leftrightarrow (v, \text{div } \mathbf{q}) = \langle g, \mathbf{q}^T \nu \rangle \quad \text{and} \quad (\text{div } \mathbf{p}, w) = 0. \quad (10)$$

Note that the term  $\langle g, \mathbf{q}^T \nu \rangle$  is independent of any integration constant for  $g$  chosen in (6) because  $\mathbf{q}^T \nu$  has average normal trace zero on  $\partial\Omega$ .

For the discretization of (10) we use the space  $\tilde{W}_h$  of piecewise constant functions with mean value zero, and the  $\tilde{\mathbf{H}}(\text{div}; \Omega)$ -conforming lowest-order Raviart-Thomas space  $\tilde{\mathbf{\Gamma}}_h$ . Recall that those spaces satisfy the Babuška-Brezzi-Ladyshenskaja condition and that  $\text{div } \tilde{\mathbf{\Gamma}}_h = \tilde{W}_h$ . Moreover,  $\tilde{\mathbf{\Gamma}}_h$  is a proper subspace of all piecewise linear vectorfields and its  $\tilde{\mathbf{H}}(\text{div}; \Omega)$ -conformity is guaranteed by continuity of the normal components of the discrete fields across the element edges. Those normal components are constants on each edge and represent the degrees of freedom.

**Remark 2.1** With the application illustrated in Figure 1 in mind, note that contour lines of a piecewise constant functions do not make much sense. In Section 3.2.4 we will describe a post-processor that maps  $v_h$  into a better approximation of  $v$ . This approximation will be continuous piecewise linear, such that its contourlines are well-defined.

With the above choice for the discrete spaces, the mixed finite element approximations  $(v_h, \mathbf{p}_h) \in \tilde{W}_h \times \tilde{\mathbf{\Gamma}}_h$  satisfy

$$(\mathbf{p}_h, \mathbf{q}_h) \Leftrightarrow (v_h, \text{div } \mathbf{q}_h) = \langle g, \mathbf{q}_h^T \nu \rangle \quad \text{and} \quad (\text{div } \mathbf{p}_h, w_h) = 0, \quad (11)$$

for all  $(w_h, \mathbf{q}_h) \in \tilde{W}_h \times \tilde{\mathbf{\Gamma}}_h$ . Since the space  $\tilde{\mathbf{\Gamma}}_h$  does not contain *all* the piecewise linear vectorfields, its approximation quality is only of order  $h$ , which is reflected in the optimal order *a priori* bound for the mixed method in case the family of partitions  $(\mathcal{T}_h)_h$  is regular,

$$\|v \Leftrightarrow v_h\|_0 + \|\mathbf{p} \Leftrightarrow \mathbf{p}_h\|_{\text{div}} \leq Ch|v|_2. \quad (12)$$

We will show an interesting relation between  $\nabla u_h$  and  $\mathbf{p}_h$  in Section 2.4. First, we recall the discrete Helmholtz decomposition of Raviart-Thomas spaces.

## 2.3 Discrete Helmholtz decomposition

A very useful property of Raviart-Thomas spaces is, that they reflect, on a discrete level, the Helmholtz decomposition of vector fields. The continuous version is well-known, and we refer to [8] for details:

$$[L^2(\Omega)]^2 = \nabla H_0^1(\Omega) \oplus \mathbf{curl } \tilde{H}^1(\Omega). \quad (13)$$

The discrete version is preluded by the property [8],

$$\mathbf{q}_h \in \tilde{\mathbf{\Gamma}}_h \text{ and } \operatorname{div} \mathbf{q}_h = 0 \Leftrightarrow \mathbf{q}_h \in \mathbf{curl} \tilde{V}_h. \quad (14)$$

Also, define an operator  $\nabla_h : \tilde{W}_h \rightarrow \tilde{\mathbf{\Gamma}}_h$  by the Riesz theorem,

$$(\nabla_h w_h, \mathbf{q}_h) = \langle w_h, \operatorname{div} \mathbf{q}_h \rangle \text{ for all } \mathbf{q}_h \in \tilde{\mathbf{\Gamma}}_h. \quad (15)$$

**Theorem 2.2** *A discrete Helmholtz decomposition for Raviart-Thomas space is given by*

$$\tilde{\mathbf{\Gamma}}_h = \nabla_h \tilde{W}_h \oplus \mathbf{curl} \tilde{V}_h. \quad (16)$$

*This decomposition is  $L^2$ -orthogonal.*

**Proof.** See also [13]. The right-hand side of (16) is clearly a subspace of  $\tilde{\mathbf{\Gamma}}_h$ . The orthogonality follows directly from (15) by substituting  $\mathbf{q}_h = \mathbf{curl} \omega_h$  and the fact that  $\operatorname{div} \mathbf{curl} = 0$ . Now, for given  $\mathbf{q}_h \in \tilde{\mathbf{\Gamma}}_h$ , let  $\mathbf{r}_h$  be its  $L^2$ -orthogonal projection on  $\nabla_h \tilde{W}_h$ , so,

$$\forall w_h \in \tilde{W}_h, \quad (\mathbf{q}_h \ominus \mathbf{r}_h, \nabla_h w_h) = 0. \quad (17)$$

Recall that  $\operatorname{div} \tilde{\mathbf{\Gamma}}_h = \tilde{W}_h$ . This, in combination with (15), gives that  $\mathbf{q}_h \ominus \mathbf{r}_h$  is divergence-free, which, by (14) implies that  $\mathbf{q}_h \ominus \mathbf{r}_h \in \mathbf{curl} \tilde{V}_h$ . So, also the reverse inclusion in (16) holds.  $\square$

## 2.4 Discrete Cauchy-Riemann relations

We will now derive some results on the standard and mixed approximations of the Cauchy-Riemann pair  $(u, v)$ . Looking at the defining equations (11) for the mixed finite element approximations, we can conclude by  $\operatorname{div} \tilde{\mathbf{\Gamma}}_h = \tilde{W}_h$  that  $\operatorname{div} \mathbf{p}_h = 0$  and therefore, by (14), that  $\mathbf{p}_h = \mathbf{curl} \omega_h$  for some  $\omega_h \in \tilde{V}_h$ . Substituting this information back into (11) gives that

$$\forall \mathbf{q}_h \in \tilde{\mathbf{\Gamma}}_h, \quad (\mathbf{curl} \omega_h, \mathbf{q}_h) \Leftrightarrow (v_h, \operatorname{div} \mathbf{q}_h) = \langle g, \mathbf{q}_h^T \nu \rangle. \quad (18)$$

By the discrete Helmholtz decomposition (16), this decouples into two independent sets of equations by testing into the two orthogonal subspaces of  $\tilde{\mathbf{\Gamma}}_h$  consecutively. This gives first of all that

$$\forall y_h \in \tilde{V}_h, \quad (\mathbf{curl} \omega_h, \mathbf{curl} y_h) = \langle g, \mathbf{curl} y_h^T \nu \rangle. \quad (19)$$

Using (4), note that  $\mathbf{curl} y_h^T \nu = \frac{\partial}{\partial \tau} y_h$ . Then, integration by parts on  $\partial\Omega$  and using (4) again to conclude that  $(\mathbf{curl} \omega_h, \mathbf{curl} y_h) = (\nabla \omega_h, \nabla y_h)$ , gives

$$\forall y_h \in \tilde{V}_h, \quad (\nabla \omega_h, \nabla y_h) = \left\langle \frac{\partial}{\partial \tau} g, y_h \right\rangle = \langle j, y_h \rangle. \quad (20)$$

Comparing this to (8) leads to the interesting observation that the Cauchy-Riemann relation  $\mathbf{p} = \mathbf{curl} u$  is reflected in the discretizations. We summarize our findings in the following theorem.

**Theorem 2.3** *Let  $u$  and  $v$  satisfy the Laplace equations (3) and (6), and let  $(u_h, \nabla u_h)$  and  $(v_h, \mathbf{p}_h)$  be the standard and mixed finite element approximations of  $(u, \nabla u)$  and  $(v, \mathbf{p} = \nabla v)$  as described by (8) and (11). Then,*

$$\mathbf{curl} u = \mathbf{p} = \nabla v \text{ and } \mathbf{curl} u_h = \mathbf{p}_h. \quad (21)$$

### 3 Fast solution, superconvergence, and error estimation

In this section we will concentrate on some issues of practical importance. Knowing that  $u_h$  and  $v_h$  satisfy the discrete Cauchy-Riemann relation (21), the question is how to compute  $v_h$  given that  $\mathbf{p}_h = \mathbf{curl} u_h$  is known. Another question is how to benefit from superconvergence of the finite element solutions.

#### 3.1 Optimal complexity solution of the missing potential

We will first describe an efficient method to solve  $v_h$  from

$$\forall \mathbf{q}_h \in \tilde{\Gamma}_h, \quad (v_h, \operatorname{div} \mathbf{q}_h) = (\mathbf{curl} u_h, \mathbf{q}_h) \Leftrightarrow \langle g, \mathbf{q}_h^T \nu \rangle, \quad (22)$$

This equation is nothing more than (11) combined with the result from Theorem 2.3 that  $\mathbf{p}_h = \mathbf{curl} u_h$ . For the practical solution of  $v_h$  from (22), it is important to see that, although  $\operatorname{div} \tilde{\Gamma}_h = \tilde{W}_h$ ,

$$\dim(\tilde{\Gamma}_h) = \dim(\mathbf{curl} \tilde{V}_h) + \dim(\nabla_h \tilde{W}_h) = \dim(\tilde{V}_h) + \dim(\tilde{W}_h) > \dim(\tilde{W}_h), \quad (23)$$

which means that (22) results in a non-square though consistent linear system of equations, which, for example, can be solved by elimination of redundant equations.

##### 3.1.1 Reducing the number of equations

An obvious way to reduce the number of equations would be to use only the subspace  $\nabla_h \tilde{W}_h \subset \tilde{\Gamma}_h$  as testspace in (22) and to solve  $v_h$  from

$$\forall w_h \in \tilde{W}_h, \quad (\nabla_h v_h, \nabla_h w_h) = \langle g, \nabla_h w_h^T \nu \rangle. \quad (24)$$

This, however, has the practical disadvantage that the operator  $\nabla_h$  is given in the form of a linear system (15), and that a local basis for  $\nabla_h \tilde{W}_h$  is not known. Therefore, the following trivial observation is important. We do not need the space  $\nabla_h \tilde{W}_h$  itself as test space. Any subspace  $\tilde{\mathbf{Z}}_h \subset \tilde{\Gamma}_h$  such that

$$\operatorname{div} : \tilde{\mathbf{Z}}_h \rightarrow \tilde{W}_h \quad \text{is a bijection} \quad (25)$$

gives rise to a non-singular square system with, henceforth, the correct solution. We will now implicitly give an example of such a subspace.

##### 3.1.2 The marching process

Let  $e$  be an internal edge of the triangulation, and  $S$  and  $T$  triangles sharing  $e$ . Let  $\mathbf{q}_e \in \tilde{\Gamma}_h$  be such that  $\mathbf{q}_e^T \nu_S = |e|^{-1}$  on  $e$ , where  $\nu_S$  points from  $S$  to  $T$ ,  $\mathbf{q}_e^T \nu = 0$  on all other edges. Define  $w_e := \operatorname{div} \mathbf{q}_e \in \tilde{W}_h$ , then by the Gauss Divergence Theorem,  $w_e = |S|^{-1}$  on  $S$  and  $w_e = \Leftrightarrow |T|^{-1}$  on  $T$ . The set

$$\mathcal{W} := \{w_e \mid e \text{ is an internal edge of the triangulation}\}, \quad (26)$$

spans  $\tilde{W}_h$ , but is, in general, not a basis for  $\tilde{W}_h$ . As depicted in Figure 2 below, simple triangulations can be found for which the number of internal edges is strictly

larger than the dimension of  $\tilde{W}_h$ , which equals the number of triangles  $T$  minus one. This can be quantified, for example, by using the discrete Helmholtz decomposition (16). The dimension of  $\tilde{\mathbf{T}}_h$  equals the total number  $E$  of edges minus one, whereas the dimension of  $\mathbf{curl} \tilde{V}_h$  equals the total number  $N$  of nodes minus one. This results in a special case of Euler's formula,

$$E = T + N \Leftrightarrow 1. \quad (27)$$

Since the numbers of boundary edges and boundary nodes coincide, this formula can also be used reading for  $E$  and  $N$  the number of internal edges and nodes.

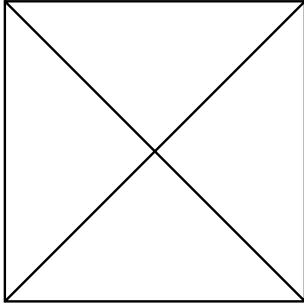


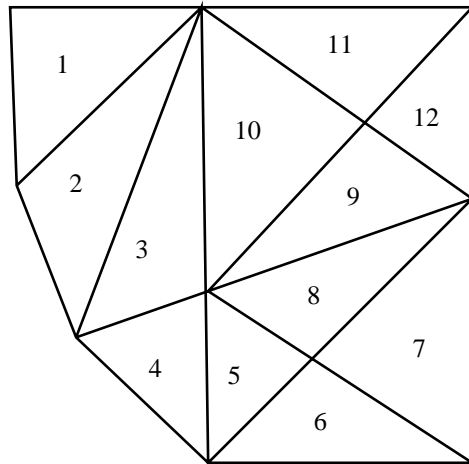
**Figure 2.** The dimension of  $\tilde{W}_h$  equals three, which is the number of triangles minus one. But there are four internal edges, so  $\mathcal{W}$  is not a basis. The functions  $w_e$  only form a basis if there are no internal nodes, as follows from (27).

A direct way to solve  $v_h$  from (22) is the so-called *marching process* (see for example [6, 16]). It is based on the fact that for each constant value  $c$ , the function  $v_h + c$  satisfies (22), which explains the start of the algorithm:

- On an arbitrary triangle, assign an arbitrary value to  $v_h$ .
- Let  $e$  be an internal edge such, that a value has been given to  $v_h$  on exactly one of the two triangles sharing  $e$ . Compute the missing value of  $v_h$  on the other triangle by testing (22) with  $\mathbf{q}_e$ .
- Repeat the second step until all triangles have been visited.
- Subtract the mean value of  $v_h$  from  $v_h$ .

An example of a “march” is given in Figure 3 below. Starting with a given value in triangle 1, a value in triangle 2 is computed, then in triangle 3, and so on.

**Figure 3.** Illustration of a marching process. Contrary to what this example may suggest, it is not necessary that triangle  $j+1$  is a neighbor of triangle  $j$ , only that it is a neighbor of triangle  $k$  for some  $k < j+1$ .



**Remark 3.1** The marching process has optimal complexity. It computes  $T \Leftrightarrow 1 := \dim(\tilde{W}_h)$  unknowns in  $\mathcal{O}(T)$  arithmetical operations.

Another important observation is that since all the functions  $\mathbf{q}_e$  in the marching process have normal trace equal to zero on  $\partial\Omega$ , we have that

$$\forall \mathbf{q}_e, \quad \langle g, \mathbf{q}_e^T \nu \rangle = 0. \quad (28)$$

so in fact we do not need to know  $g$  at all. Concretely,  $v_h$  is computed from

$$\forall q_h \in \tilde{\mathbf{Z}}_h \subset \tilde{\mathbf{\Gamma}}_h, \quad (v_h, \operatorname{div} \mathbf{q}_h) = (\mathbf{curl} u_h, \mathbf{q}_h), \quad (29)$$

so apparently,  $u_h$  contains all information from the boundary data necessary to compute  $v_h$ . Note that the evaluation of both terms in (29) can be done exactly, for example by numerical integration. Denoting the two triangles sharing an edge  $e$  by  $S$  and  $T$  and their centers of gravity by  $P$  and  $Q$ , the midpoint rule gives

$$(v_h, \operatorname{div} \mathbf{q}_e) = v_h(S) \Leftrightarrow v_h(T), \quad \text{and} \quad (30)$$

$$(\mathbf{curl} u_h, \mathbf{q}_e) = |S| \mathbf{curl} u_h^T \mathbf{q}_e(P) + |T| \mathbf{curl} u_h^T \mathbf{q}_e(Q). \quad (31)$$

### 3.1.3 The marching process for exactly given $\mathbf{curl} u$

So far, we have assumed that approximations for  $u$  became available through standard finite element approximation. In some applications, it might happen that  $u$  is known *a priori*. In that case, note that (29) still defines a valid discretization, since the matrix corresponding to the left-hand side is still invertible. Moreover, since we know that  $\mathbf{curl} u = \Leftrightarrow \nabla v$ , it follows that  $v_h$  satisfies

$$\forall q_h \in \tilde{\mathbf{Z}}_h \subset \tilde{\mathbf{\Gamma}}_h, \quad (v_h, \operatorname{div} \mathbf{q}_h) = \Leftrightarrow (\nabla v, \mathbf{q}_h) = (v, \operatorname{div} \mathbf{q}_h). \quad (32)$$

So, this discretization yields the optimal approximation  $v_h := P_h v$ , where  $P_h$  is the  $L^2$ -orthogonal projection on  $\tilde{W}_h$ . The use of quadrature for the evaluation of the right-hand side  $(\mathbf{curl} u, \mathbf{q}_h)$  could damage this property.

### 3.1.4 The effects of numerical integration and algebraic errors

In numerical practice, the standard finite element solution  $u_h$  needs to be solved from a linear system of equations. This may introduce an algebraic error in  $u_h$ , resulting in an approximation  $\hat{u}_h$  of  $u_h$ . Apart from that, numerical integration might have been used to compute the right-hand side of (8). Consequently, (22) will in general only have a solution in the least-squares sense. The marching process, however, can still be applied without modification. As a matter of fact, it then approximates the solution to this least-squares problem by selecting a number of  $T \Leftrightarrow 1 := \dim(\tilde{W}_h)$  equations from the overdetermined system (22), and to solve those exactly.

**Remark 3.2** A similar process is known in the context of numerical linear algebra<sup>1</sup>. Suppose  $\lambda$  is an eigenvalue of an  $n \times n$  matrix  $A$  and that for  $v \neq 0$ ,  $(A \Leftrightarrow \lambda I)v = 0$ .

<sup>1</sup>I thank Michiel Hochstenbach and Jasper van den Eshof for pointing out this similarity

Assume that  $\lambda$  is single, then  $\text{rank}(A \Leftrightarrow \lambda I) = n \Leftrightarrow 1$  so all entries of  $v$  must be non-zero. Now, fix an entry  $v_j$  of  $v$ , and bring  $v_j$  times the  $j$ -th column of  $A \Leftrightarrow \lambda I$  to the right hand side. What remains is an overdetermined though consistent linear system for the remaining  $n \Leftrightarrow 1$  entries of  $v$ . In case merely an approximation  $\hat{\lambda}$  of  $\lambda$  is known, Wilkinson suggests in his 1958 paper [17] to use the same procedure. Move one column of the matrix  $A \Leftrightarrow \hat{\lambda} I$  to the right-hand side and solve the least-squares problem that remains by selecting  $n \Leftrightarrow 1$  equations. In case of a tridiagonal matrix  $A$ , this solution process can be done in optimal complexity (approximately  $3n$  operations) by forward substitution.

From numerical linear algebra point of view, it is known that procedures like these, can result in a non-optimal approximate solution. A safe way out would be to give up the optimal complexity and to solve the least squares system by  $QR$ -factorization or by using the normal equations.

### 3.1.5 A note on stability of marching processes

The stability of the marching process depends very much on which march is chosen, but also on the distribution over the domain of the perturbation of the right-hand side. The march as illustrated in Figure 3 is one long march, which means that errors are accumulated along the whole trajectory. A better march would be to start somewhere in the center of the domain, compute new values for all three adjacent triangles, then all triangles adjacent to those four, etcetera. In Figure 3 this would be: start with 10, compute 3,9,11 from 10, compute 2,4,8,12, then 1,5,7, and finally 6. The maximum error accumulation trajectories would then have a length that is of the order of the square root of the length of the march given in Figure 3. The analysis of a march could follow from the error equation

$$\forall \mathbf{q}_h \in \tilde{\mathbf{Z}}_h \subset \tilde{\mathbf{\Gamma}}_h, \quad (\hat{v}_h \Leftrightarrow v_h, \text{div } \mathbf{q}_h) = (\mathbf{curl}(\hat{u}_h \Leftrightarrow u_h), \mathbf{q}_h) \quad (33)$$

where  $\hat{u}_h$  is the approximation of  $u_h$  obtained by the finite element method, which can contain errors due to numerical integration and inexact solution of the linear system. From (33) it follows that

$$\|\hat{v}_h \Leftrightarrow v_h\|_0 \leq \sup_{0 \neq \mathbf{q}_h \in \tilde{\mathbf{Z}}_h} \frac{\|\mathbf{q}_h\|_0}{\|\text{div } \mathbf{q}_h\|_0} \|\mathbf{curl}(\hat{u}_h \Leftrightarrow u_h)\|_0, \quad (34)$$

which involves the operator norm of the inverse of the divergence seen as operator from  $\tilde{W}_h$  to  $\tilde{\mathbf{Z}}_h$ , and  $\tilde{\mathbf{Z}}_h$  the subspace of  $\tilde{\mathbf{\Gamma}}_h$  corresponding to the march. Clearly, an analysis independent of the march would lead to upper bounds for the error propagation that would be an overestimation for a specific march. On the other hand, analyzing a specific march is not very hard but we do not want to specify the form of the domain and its triangulation. We will just present one line of reasoning here for illustration.

A local bound follows already directly from (33) in combination with (30). Writing  $a_h = v_h \Leftrightarrow \hat{v}_h$  for the error, we get, using that  $\|\mathbf{q}_e\|_{0,T \cup S} \leq C$  on regular families of partitions, that

$$|a_h(S) \Leftrightarrow a_h(T)| \leq C \|\mathbf{curl}(u_h \Leftrightarrow \hat{u}_h)\|_{0,T \cup S}. \quad (35)$$

So the difference between the errors on two arbitrary triangles  $A$  and  $B$  is bounded by the accumulation of those local bounds over the shortest possible trajectory from  $A$  to  $B$ . We prefer to minimize the length of the trajectory instead of minimizing the local errors, since the latter are basically unknown. The result is that

$$|a_h(A) \Leftrightarrow a_h(B)| \leq C \sum_{k=1}^N \|\mathbf{curl}(u_h \Leftrightarrow \hat{u}_h)\|_{0,T_k} \leq C\sqrt{N} \|\mathbf{curl}(u_h \Leftrightarrow \hat{u}_h)\|_{0,X}, \quad (36)$$

where  $N$  is the number of triangles  $T_k$  on the shortest path in the marching process between  $A$  and  $B$ , and  $X$  denotes their union. Since  $a_h$  has mean value zero, we conclude the second inequality in

$$\|a_h\|_0 \leq C \|a_h\|_\infty \leq C \max_{A,B \in \mathcal{T}_h} |a_h(A) \Leftrightarrow a_h(B)|. \quad (37)$$

For the long march from Figure 3, which uses all  $\mathcal{O}(h^{-2})$  elements, triangles nr. 1 and nr. 12 maximize the expression in the right-hand side of (37), which leads to the upper bound,

$$\|\hat{v}_h \Leftrightarrow v_h\|_0 \leq Ch^{-1} \|\mathbf{curl}(u_h \Leftrightarrow \hat{u}_h)\|_{0,\Omega}, \quad (38)$$

because the trajectory from  $A$  to  $B$  covers the whole domain. In case the paths are shorter, like suggested earlier in this section, we need to assume that the errors in  $\hat{u}_h$  are distributed equally over the domain, as holds for the finite element error. In that case we get, with  $\mathcal{O}(h^{-1})$  elements and  $Y$  the corresponding portion of  $\Omega$ ,

$$\|\hat{v}_h \Leftrightarrow v_h\|_0 \leq Ch^{-\frac{1}{2}} \|\mathbf{curl}(u_h \Leftrightarrow \hat{u}_h)\|_{0,Y} \leq C \|\mathbf{curl}(u_h \Leftrightarrow \hat{u}_h)\|_{0,\Omega}. \quad (39)$$

The bounds show that to obtain the optimal *a priori* approximation quality of  $v_h$ , it is necessary to solve  $u_h$  with an algebraic error in the same order of magnitude as its discretization error in case the latter march-type is employed, or one order higher if the simple long march type of Figure 3 is used.

## 3.2 Superconvergence based a posteriori error estimation

In standard as well as in mixed finite elements, superconvergence results are known that may help to post-process the discrete solutions and to estimate the error *a posteriori*. Because of the discrete Cauchy-Riemann relation of Theorem 2.3, superconvergence properties of the one method can in fact be derived from superconvergence of the other. We will therefore start with recalling superconvergence results for the standard finite element method. Then we apply them to the Laplace equation and finally transfer them to the mixed approximations.

### 3.2.1 Historic remarks and sketch of the main idea

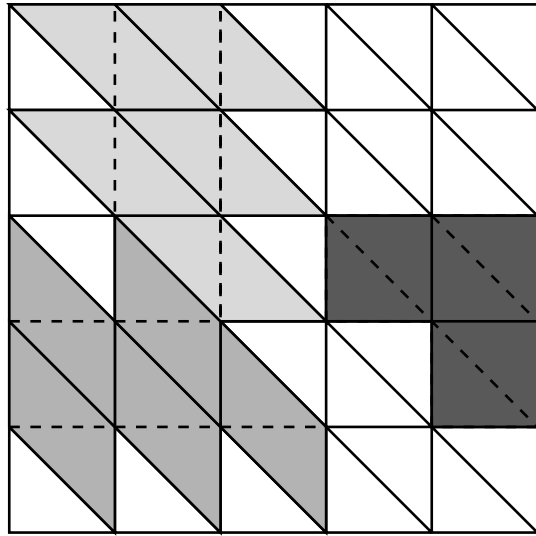
Already in 1969, Oganjesjan and Ruhovets [12] proved superconvergence for the linear finite element method applied to the Poisson problem with homogeneous Dirichlet boundary conditions and on uniform triangular partitions. Recall that uniform partitions are also called *three-directional* because the directions of the edges of each triangle are the same. Oganjesjan and Ruhovets showed that the gradient of

the continuous linear finite element approximation  $u_h$ , is closer to the gradient of the linear Lagrange interpolants  $L_h u$  of  $u$  than to the exact solution  $\nabla u$ . Explicitly,

$$\|\nabla(u_h \Leftrightarrow L_h u)\|_0 \leq Ch^2|u|_3, \quad (40)$$

whereas both  $\nabla u_h$  and  $\nabla L_h u$  approximate  $\nabla u$  only with order  $\mathcal{O}(h)$ . This supercloseness is due to the key property that derivatives in the mesh directions of functions from the space  $V_{0h}$  of continuous piecewise linear functions that are zero on the boundary, are piecewise constant functions on parallelograms, and zero on remaining boundary triangles, as depicted in Figure 4 below.

**Figure 4.** The tangential derivative along a dashed edge of a continuous piecewise linear function  $y_h$  is constant on the parallelogram formed by the two triangles sharing that edge. The union of all parallelograms over all internal edges in a given direction covers omega, apart from some triangles at the boundary. If  $y_h$  is zero on  $\partial\Omega$ , then so is its tangential derivative on those boundary triangles.



This property holds in particular for functions  $L_h p \in V_{0h}$  where  $p$  is a quadratic function. If  $p$  is quadratic, it is moreover easy to check that given an edge  $e$  with midpoint  $M$  and a vector  $\tau$  tangential to  $e$ ,

$$\frac{\partial}{\partial \tau} L_h p(M) = \frac{\partial}{\partial \tau} p(M), \quad (41)$$

Since  $\frac{\partial}{\partial \tau} L_h p(M)$  is constant and  $\frac{\partial}{\partial \tau} p(M)$  linear on the parallelogram  $N$  around  $e$ , we get

$$\left(\frac{\partial}{\partial \tau}(p \Leftrightarrow L_h p), 1\right)_N = 0. \quad (42)$$

This property enables the local application of the Bramble-Hilbert lemma, and this results in

$$\forall y_h \in V_{0h}, \quad |(\nabla u \Leftrightarrow \nabla L_h u, \nabla y_h)| \leq Ch^2|u|_3|\nabla y_h|_0, \quad (43)$$

from which (40) can be derived through Galerkin orthogonality. We refer to [12] for details.

**Remark 3.3** The regularity assumption  $u \in \tilde{H}^3(\Omega)$  cannot be obtained by demanding higher regularity of  $j$  because  $\partial\Omega$  is not smooth enough. However,  $u \in \tilde{H}^{5/2}(\Omega)$  is possible. Moreover, restricted to interior triangles,  $u$  will be smooth enough. Application of the Bramble-Hilbert lemma will be possible apart from a strip  $\Omega_h$  of

width order  $h$  along the boundary. On this strip the bound  $|z|_{0,\Omega_h} \leq C\sqrt{h}|z|_{1/2,\Omega_h}$  can be used. This results in a total bound of order  $\mathcal{O}(h\sqrt{h})$ , just as for the Laplace problem that we will consider now.

### 3.2.2 Supercloseness in the Laplace problem

For the Laplace problem (3) and its discretization (7), the situation is slightly more complicated as a result of the non-homogeneous boundary conditions. There exist boundary triangles, on which the directional derivatives of functions from  $\tilde{V}_h$  do not vanish. Application of the Bramble-Hilbert lemma is there not possible, basically because integrals of functions that are odd around the center of gravity of a single triangles do not vanish. Fortunately, there are not many boundary triangles, and the result (derived by several authors, see for example [11] for a review) is that merely

$$\forall y_h \in \tilde{V}_h, \quad |(\nabla u \Leftrightarrow \nabla L_h u, \nabla y_h)| \leq Ch\sqrt{h} \left( |u|_{\frac{5}{2},\Omega_h} + |u|_{3,\Omega \setminus \Omega_h} \right) |\nabla y_h|_0, \quad (44)$$

which gives a supercloseness of magnitude

$$\|\nabla(u_h \Leftrightarrow L_h u)\|_0 \leq Ch\sqrt{h} \left( |u|_{\frac{5}{2},\Omega_h} + |u|_{3,\Omega \setminus \Omega_h} \right). \quad (45)$$

### 3.2.3 Postprocessing and error estimation

The supercloseness result (45) for the Laplace problem, though less super than in (40), can still be effectively used to post-process the gradient approximation. There are several possibilities to do so, but each one of them is based on (41). So, on a triangle  $T$ , three parameters of the five that uniquely determine  $\nabla p$  on  $T$  can be directly found from  $\nabla L_h p$  only. Thus, combining information from several neighboring triangles,  $\nabla p$  can be recovered exactly. This is illustrated in Figure 5, where a post-processing scheme is depicted that exactly recovers  $\nabla p(N)$  at some node  $N$ .

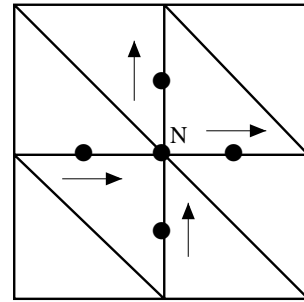


**Figure 5.** The average of two exact tangential derivatives in the same direction gives the exact derivative in that direction at the node  $N$ . The gradient can be recovered by doing this for two independent, not necessarily orthogonal, directions.

Let  $K_h : \nabla \tilde{V}_h \rightarrow [V_h]^2$  be the operator of which the nodal values are determined by this process. So, at an internal node, the value of  $K_h y_h$  is computed by averaging of tangential components at midpoints of edges as in Figure 5. At boundary nodes, use extrapolation of recovered values at nearby internal nodes. The result will be that

$$\|\nabla u \Leftrightarrow K_h \nabla u_h\|_0 \leq Ch\sqrt{h} \left( |u|_{\frac{5}{2},\Omega_h} + |u|_{3,\Omega \setminus \Omega_h} \right). \quad (46)$$

Consequently, the difference  $\varepsilon(h)$  between the post-processed approximation  $K_h \nabla u_h$  and the original approximation  $\nabla u_h$  will be an asymptotically exact *a posteriori* error estimator for the error  $\|\nabla u \Leftrightarrow \nabla u_h\|_0$ ,

$$\varepsilon(h) := \|(I \Leftrightarrow K_h) \nabla u_h\|_0 \quad \text{and} \quad \eta(h) := \frac{\varepsilon(h)}{\|\nabla u \Leftrightarrow \nabla u_h\|_0} \rightarrow 1, \quad (h \rightarrow 0). \quad (47)$$

### 3.2.4 Supercloseness for the mixed method

Consider the mixed discretization (11) of Laplace problem (6). We have proved in Section 2.4 a discrete Cauchy-Riemann relation stating that  $\mathbf{p}_h = \mathbf{curl} u_h$ . From this and the results of the previous section for  $\nabla u_h$ , we conclude easily that  $\varepsilon(h)$  is also an asymptotically exact *a posteriori* error estimator for the error  $\|\Leftrightarrow \nabla v \Leftrightarrow \mathbf{p}_h\|_0$ , and that

$$\varepsilon(h) := \|(I \Leftrightarrow K_h) \nabla u_h\|_0 = \|(I \Leftrightarrow \hat{K}_h) \mathbf{p}_h\|_0, \quad (48)$$

where  $\hat{K}_h : \tilde{\mathbf{T}}_h \rightarrow [V_h]^2$  is the similarly derived recovery operator for the exact normal components instead of for the tangential components. So,  $\hat{\varepsilon}(h)$  can be computed in the mixed setting directly from  $\mathbf{p}_h$ . Note that the recovery operator  $\hat{K}_h$  was introduced in [4] for mixed approximation of elliptic equations. We have shown now that for the Laplace equation it is equivalent to  $K_h$ .

The most interesting question is of course how to profit from superconvergence when the mixed approximation  $v_h$  of  $v$  is under consideration. This is answered by the following result by Douglas and Roberts [7], which states that on regular families of possibly non-uniform partitions,

$$\|P_h v \Leftrightarrow v_h\|_0 \leq Ch^2 |v|_2, \quad (49)$$

where  $P_h$  stands for the  $L^2$ -orthogonal projection on  $\tilde{W}_h$ . This supercloseness gives rise to a post-processing scheme  $Q_h$  defined by averaging at nodes of the constant values on all triangles sharing that node, followed by interpolation on those averaged values by continuous piecewise linear functions. This results in

$$\|v \Leftrightarrow Q_h v_h\|_0 \leq Ch^2 |v|_2. \quad (50)$$

Similar as for the vector fields, this gives rise to an asymptotically exact *a posteriori* error estimator  $\gamma(h)$  for the original error in  $v_h$ ,

$$\gamma(h) := \|(I \Leftrightarrow Q_h) v_h\|_0 \quad \text{and} \quad \xi(h) := \frac{\gamma(h)}{\|v \Leftrightarrow v_h\|_0} \rightarrow 1, \quad (h \rightarrow 0). \quad (51)$$

Contour lines of the post-processed solution  $Q_h v_h$  will be continuous and piecewise linear, whereas contour lines for  $v_h$  do not make sense. So apart from the fact that  $Q_h$  is a higher order approximation to  $v$  than  $v_h$ , it also allows the application described in the Introduction of this paper. Note that no special grid structure is required for this post-processing, so that adaptive and local refinement can take place that is based on information supplied by the error estimator.

**Remark 3.4** To guarantee the superconvergence in  $v_h$ , it is necessary to solve  $u_h$  with an algebraic error that is superconvergent, i.e., one order higher than the approximation error of  $u_h$ . Then, the marching process from Section 3.1.5 should be used.

## 4 Conclusions

We have developed a complete package for the approximation of the Cauchy-Riemann equations. Firstly, we showed a discrete Cauchy-Riemann relation that was valid for the standard and mixed finite element discretizations of the unknown functions. Secondly, we concentrated on the practical computation of one as by-product of the computation of the other one. Thirdly, we concluded that superconvergence properties from standard finite elements automatically get transferred to the mixed elements. Using the superconvergence, the error in the gradient, the curl, and one of the potentials can be estimated *a posteriori*, and grid refinement could be applied.

## Acknowledgments

The research leading to this paper was supported by a Research Fellowship of the Royal Netherlands Academy of Arts and Sciences. This support is gratefully acknowledged. Moreover, the author thanks Rob Stevenson for useful suggestions and discussions in the context of the topic of this paper.

## References

- [1] A. Borzi, K.W. Morton, E. Süli and M. Vanmeale (1997). Multilevel solution of cell vertex Cauchy-Riemann equations. *SIAM J. Sci. Comp.*, 18:441–459.
- [2] D. Braess and R. Verfürth (1996). A posteriori error estimation for the Raviart-Thomas element. *SIAM J. Numer. Anal.*, 33:2431–2444.
- [3] A. Brandt and N. Dinar (1979). *Multigrid solutions to elliptic flow problems*, in Numerical methods for partial differential equations, S.V. Parter, ed. Academic Press, New York.
- [4] J.H. Brandts (1994). Superconvergence and a posteriori error estimation in triangular mixed finite elements. *Numer. Math.*, 68(3):311–324.
- [5] P. Ciarlet (1978). *The finite element method for elliptic problems*. North-Holland, Amsterdam.
- [6] C. Cuvelier, A. Segal, and A. van Steenhoven (1986). *Finite element methods and Navier-Stokes equations*. D. Reidel Publishing Company, Dordrecht, Netherlands.
- [7] J. Douglas and J.E. Roberts (1985). Global estimates for mixed methods for second order elliptic problems. *Math. Comp.*, 44(169):39–52.
- [8] V. Girault and P.A. Raviart (1986). *Finite element methods for Navier-Stokes equations. Theory and algorithms*. Springer Series in Computational Mathematics, Springer-Verlag, Berlin Heidelberg.
- [9] M. Ghil and R. Balgovid (1979). A fast Cauchy-Riemann solver. *Math. Comp.*, 33:585–635.

- [10] W. Hackbusch (1986). *Theorie und Numerik elliptischer Differentialgleichungen*. B.G. Teubner, Stuttgart.
- [11] M. Krizek and P. Neittaanmäki (1987). On superconvergence techniques. *Acta Appl. Math.*, 9:175–233.
- [12] L.A. Oganessian and L.A. Ruhovets (1969). Study of the rate of convergence of variational difference schemes for second-order elliptic equations in a two-dimensional field with a smooth boundary. *Ž. Vyčisl. Mat. i Mat. Fiz.*, 9:1102–1120.
- [13] P. Peisker and D. Braess (1992). Uniform convergence of mixed interpolated elements for Reissner-Mindlin plates. *RAIRO Modél. Math. Anal. Numér.*, 26:557–574.
- [14] P.A. Raviart and J.M. Thomas (1977). A mixed finite element method for  $2^{nd}$  order elliptic problems. *Lecture Notes in Mathematics*, 606:292–315.
- [15] S. Ta'asan (1993). *Canonical forms of multidimensional steady inviscid flows*. ICASE 93-34, Institute for Computer Applications in Science and Engineering, Hampton, VA.
- [16] S. Turek (1994). Multigrid techniques for a divergence-free finite element discretization. *East-West J. Numer. Math.*, 2:229–255.
- [17] J. Wilkinson (1958). The calculation of eigenvectors of codiagonal matrices. *Computer J.*, 1:90–96.